Science of the Total Environment 871 (2023) 162037

Contents lists available at ScienceDirect

Science of the Total Environment

journal homepage: www.elsevier.com/locate/scitotenv

An improved Chemcatcher-based method for the integrative passive sampling of 44 hydrophilic micropollutants in surface water – Part A: Calibration under four controlled hydrodynamic conditions

Vick Glanzmann [a,*], Naomi Reymond [a], Céline Weyermann [a,*], Nicolas Estoppey [a,b]

[a] School of Criminal Justice, University of Lausanne, Batochime building, 1015 Lausanne, Switzerland
[b] Norwegian Geotechnical Institute (NGI), P.O. Box. 3930 Ullevål Stadion, N-0806 Oslo, Norway

HIGHLIGHTS

- Calibration of Chemcatcher-like passive samplers at four hydrodynamic conditions
- Measurement of the four mass transfer coefficients of the water boundary layer (k_w)
- Relationships between k_w and the sampling rate (R_s) for 44 hydrophilic compounds
- Adapted model for mixed rate control by the membrane and the water boundary layer
- Relationships between k_w and R_s allow determining in-situ R_s from k_w measurements.

GRAPHICAL ABSTRACT

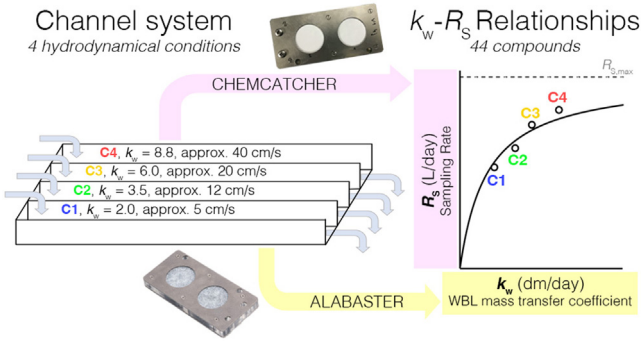

ARTICLE INFO

Editor: Damia Barcelo

Keywords:
Chemcatcher
Environmental chemistry
Water quality monitoring
Organic contaminants
Liquid chromatography

ABSTRACT

When monitoring water quality with hydrophilic integrative passive sampling devices, it is crucial to use accurate sampling rates (R_S) that account for exposure conditions such as hydrodynamics. This study aims at calibrating Chemcatcher-like passive samplers – styrene-divinylbenzene reverse phase sulfonate (SDB-RPS) extraction disk covered by a polyethersulfone (PES) membrane – at four water flow velocities (5 to 40 cm s^{-1}) in a channel system. First, the four hydrodynamic conditions were characterized by measuring the mass transfer coefficients of the water boundary layer (k_w) at the surface of the samplers using the alabaster dissolution method. Then, fifty-six samplers were deployed in the channels and exposed for 7 different intervals varying from 1 to 21 days. Thus, R_S were determined at four different k_w for 44 hydrophilic compounds, ranging from 0.015 to 0.115 L day^{-1}. Relationships were established between k_w and R_S using models for mixed rate control by the membrane and the water boundary layer. The estimated parameters of those relationships are suitable for the determination of accurate R_S when k_w is measured in situ, for example by co-deploying silicone disks spiked with performance and reference compounds (PRC) as implemented in Part B.

1. Introduction

Over the last decades, water pollution has become a great concern in our societies. Due to climate change and population increase, this problem may become one of the major challenges humanity will be facing in the future (Schwarzenbach et al., 2010; Fang et al., 2019). Thus, it is crucial to control water quality with appropriate monitoring programs in order to

* Corresponding authors.
E-mail addresses: vick.glanzmann@unil.ch (V. Glanzmann), celine.weyermann@unil.ch (C. Weyermann).

http://dx.doi.org/10.1016/j.scitotenv.2023.162037
Received 24 November 2022; Received in revised form 14 January 2023; Accepted 1 February 2023
Available online 4 February 2023

protect human health, wildlife and ecosystems. Data generated during surveillance campaigns are essential to detect the most vulnerable water bodies, prioritize their surveillance, define actions to minimize pollution sources and evaluate the effectiveness of those actions (Hirsch et al., 2006; Behmel et al., 2016).

Aquatic passive sampling, based on the free flow of contaminants from water to a receiving phase as a result of a difference in chemical potentials, is an attractive option to conduct representative monitoring campaigns (Alvarez et al., 2005; Salim and Górecki, 2019). When used in the integrative sampling phase (i.e., the period during which contaminants uptake into the sampler is predominant and release of a chemical from the sampler is negligible), passive sampling devices (PSDs) allow to determine time-weighted average (TWA) concentrations of contaminants from the amount of analytes accumulated in the PSDs using an appropriate sampling rate (R_S) (Vrana et al., 2005; Vermeirssen et al., 2009). Depending on compounds properties (e.g., hydrophobicity) and environmental factors (e.g., hydrodynamic conditions and temperature), R_S can be influenced by the diffusion through different phases which are i) the water boundary layer (WBL), ii) biofilm, iii) membrane and iv) the sampler sorbent (Huckins et al., 2006; Booij et al., 2007; Mutzner et al., 2019). The resistance in WBL is influenced by hydrodynamics (i.e., WBL thickness decreases when water flow velocity increases), and many studies have shown that the accumulation rate increases with water flow velocity, with a maximum R_S ($R_{S,max}$) reached at high velocities (Vermeirssen et al., 2008; Vermeirssen et al., 2009; Li et al., 2010; Harman et al., 2012; Lissalde et al., 2016; Booij and Chen, 2018). In situ conditions are often within the range of velocities where hydrodynamics effects on R_S persist. Thus, the transfer of hydrophilic compounds may be (at least partially) under WBL control during monitoring campaigns (Harman et al., 2012; Fauvelle et al., 2017).

Because robust R_S are critical for reliable quantification of contaminants in water, it is essential to find a solution to account for the influence of hydrodynamics. For hydrophobic samplers (e.g., silicone or low-density polyethylene sheets), the use of performance and reference compounds (PRC) allows determining site-specific R_S that takes the environmental conditions into account (Booij and Smedes, 2010). For hydrophilic samplers (e.g., the polar organic compound integrative sampler, POCIS or the polar version of Chemcatcher), the use of PRC does not seem to be reliable because uptake and release of chemicals are anisotropic with those PSDs (Shaw et al., 2009; Harman et al., 2011; Mills et al., 2014). Currently, the common approach for hydrophilic samplers is to use R_S that have been previously determined during calibration studies where PSDs are exposed to contaminated water and the accumulation rate of the sampler is monitored (Li et al., 2010; Lissalde et al., 2011; Mutzner et al., 2019; Mutzner et al., 2020). To determine accurate R_S, it is thus essential to calibrate the PSDs under controlled conditions that are as close as possible to environmental conditions (e.g., water flow velocity, temperature and pH). As flow conditions are difficult to estimate either in the field or in laboratories, Booij et al. (2017) suggested to use the mass transfer coefficient of the WBL (k_w) to provide a robust characterization of the effects of hydrodynamics on the uptake of polar compounds by PSDs. The use of controlled k_w conditions during calibration experiments as well as the measurement of k_w in the field would help to choose the most accurate R_S that applies in a specific situation, leading to more accurate TWA concentration of contaminants. It also provides a better comparison basis between studies conducted at different exposure conditions (Booij et al., 2017).

In Glanzmann et al. (2022), two different methods have been proposed to measure k_w applied to Chemcatcher-type housings, the alabaster dissolution method and the PRC dissipation from silicone disks. Both have proven to be reliable to obtain accurate k_w measurements. The former is more suitable for laboratory experiments under stable conditions and the latter is adequate for field measurements where samplers are typically deployed over a few weeks.

This study aims at improving current passive sampling of hydrophilic contaminants by developing and evaluating a promising solution to determine exposure-specific R_S for Chemcatcher-like samplers. The method is based on a device that allows co-deployment of (i) a solid phase extraction disk (to accumulate hydrophilic compounds), and (ii) an alabaster plate or a PRC-spiked silicone disk (to measure k_w in laboratory and field experiments, respectively). In the first part of this paper (part A), the calibration of hydrophilic samplers, constituted of a SDB-RPS (styrene-divinylbenzene reverse phase sulfonate) disk covered by a PES (polyethersulfone) membrane, was conducted for 44 compounds at four water velocities (5 to 40 cm s^{-1}) in a channel system. Measurements of k_w were done using the alabaster dissolution method and R_S were determined using a first order uptake model (Huckins et al., 2006). Obtained R_S were used to investigate the effect of hydrodynamics on the uptake. Relationships between R_S and k_w were established by applying a model for mixed rate control by the membrane and the WBL (MRC model) and by adapting this model to better describe the obtained calibration data (adapted MRC model).

In the second part of this article (part B), the method was tested by co-deploying PRC-spiked silicone disks with hydrophilic samplers (Supplementary information SI, Fig. S1.1) in a Swiss river to measure in-situ k_w and thus estimate site-specific R_S from the previously established k_w-R_S relationships. The TWA concentrations derived from the amount of analytes accumulated in the PSDs were compared with the aqueous concentrations obtained by the local environmental agency (Direction Générale de l'Environnement, canton de Vaud, Switzerland) using composite sampling over 14 days. The obtained results and potential for a practical implementation are discussed.

2. Materials and methods

2.1. Materials

HPLC grade acetonitrile, acetone, methanol and water were obtained from Sigma-Aldrich (Switzerland). Standard solutions of analytes were purchased from Neochema (Germany) and deuterated internal standards from HPC Standard (Germany). Solid standards used to spike the water of the calibration channel system were provided by Sigma-Aldrich (Switzerland). The alabaster disks were purchased from PaSOC (The Netherlands). The Chemcatcher-like samplers were constituted of a 47 mm diameter styrene-divinylbenzene reverse phase sulfonate (SDB-RPS) extraction disk (Affinisep, France) covered by a PES membrane (pore size 0.1 μm, 47 mm diameter; PALL Scientific, USA). The home-made designed sampler holders were laser-cut from 2 mm thick stainless steel (Techniques-Laser SA, Switzerland).

2.2. Analytes of interest

The contaminants (see list in Table 1) were selected based on the following characteristics: i) mainly hydrophilic compounds ($\log K_{OW} < 5$; e.g., pesticides, pharmaceuticals), ii) frequently found in Swiss surface water (Schymanski et al., 2014; Doppler et al., 2017; Langer et al., 2017; Spycher et al., 2018), and iii) previously studied in passive sampling literature (Shaw et al., 2009; Shaw and Mueller, 2009; Vermeirssen et al., 2009; O'Brien et al., 2011a; Vermeirssen et al., 2012; Moschet et al., 2015).

2.3. Experimental setup

Calibration of the passive samplers was conducted in a 4-channel system (SI, Fig. S1.2) running with water from Lake Geneva (Switzerland) as described in Glanzmann et al. (2022). The water was re-circulated in the system and continuously refreshed with lake water at a rate of approximately 0.4 L min^{-1}, leading to a complete renewing of the water (450 L) within 1 day. A logger was installed to monitor the pH and temperature during the experiment (Multiline Multi 3620 IDS, WTW, USA). Both parameters remained constant during the experiment (pH 8.1 ± 0.1; temperature 11 ± 0.2 °C).

Five days before starting the experiment (to equilibrate the system), target compounds dissolved in methanol were added to the system (0.6 L

Table 1
Sampling rates (R_S) determined in channels 1 to 4, modelized $R_{S,max}$ obtained with the MRC model and a values and $R_{S,max}$ obtained with the adapted MRC model, for 44 compounds.

	CAS no.	logK_{ow}[a]	R_S at day 14 (L day^{-1}) for channel				MRC model	Adapted MRC model	
			1	2	3	4	$R_{S,max}$ (L day^{-1})	a	$R_{S,max}$ (L day^{-1})
2,4-D	94-75-7	−0.8 (−5.4)	0.040	0.045	0.042	0.048	0.047	1.134	0.048
5MethylBenzotriazole	136-85-6	1.61	0.064	0.069	0.067	0.076	0.077	0.893	0.076
Atrazine	1912-24-9	2.6	0.075	0.077	0.083	0.105	0.101	1.412	0.108
Bentazon	25057-89-0	2.34	0.046	0.049	0.046	0.055	0.054	0.885	0.053
Benzotriazole	95-14-7	1.44	0.046	0.041	0.045	0.050	0.048	0.762	0.048
Boscalid	188425-85-6	3	0.030	0.036	0.043	0.048	0.043	4.430	0.058
Caffeine	58-08-2	−0.07	0.044	0.053	0.051	0.058	0.057	1.698	0.061
Carbamazepine	298-46-4	2.45	0.088	0.095	0.092	0.109	0.117	0.620	0.109
Carbendazim	10605-21-7	1.52	0.056	0.062	0.063	0.075	0.072	1.583	0.077
Chloridazon	1698-60-8	1.14	0.079	0.099	0.098	0.115	0.119	1.282	0.125
Chlorotoluron	15545-48-9	2.41	0.041	0.047	0.053	0.066	0.058	3.543	0.076
Cyproconazol	94361-06-5	3.1	0.064	0.071	0.072	0.088	0.087	1.229	0.091
DEET	134-62-3	2.02	0.090	0.098	0.098	0.100	0.116	0.377	0.104
Diazinon	333-41-5	3.81 (−1.7)	0.015	0.020	0.039	0.047	0.033	15.617	0.168
Diclofenac (acid)	15307-86-5	4.51 (0.66)	0.060	0.069	0.069	0.081	0.081	1.256	0.085
Dimethenamid	87674-68-8	2.2	0.101	0.096	0.103	0.111	0.127	0.262	0.109
Dimethoate	60-51-5	0.8	0.085	0.098	0.096	0.094	0.111	0.383	0.100
Diuron	330-54-1	2.68	0.021	0.029	0.033	0.039	0.033	7.737	0.050
Ethofumesate	26225-79-6	2.7	0.031	0.044	0.047	0.055	0.049	4.173	0.068
Flufenacet	142459-58-3	3.2	0.051	0.057	0.061	0.070	0.068	1.667	0.075
Foramsulfuron	173159-57-4	−0.8	0.027	0.032	0.024	0.025	0.028	0.100	0.027
Imidacloprid	105827-78-9	0.6	0.071	0.092	0.087	0.102	0.105	1.240	0.109
Iprovalicarb	140923-17-7	3.2	0.063	0.067	0.072	0.075	0.080	0.820	0.078
Isoproturon	34123-59-6	2.87	0.055	0.060	0.065	0.078	0.074	1.881	0.083
MCPA	94-74-6	−0.8 (−5.1)	0.042	0.047	0.043	0.050	0.049	0.991	0.049
Metalaxyl-M	70630-17-0	1.8	0.040	0.078	0.087	0.094	0.090	3.528	0.137
Metamitron	41394-05-2	0.83	0.064	0.074	0.075	0.088	0.087	1.465	0.093
Metazachlor	67129-08-2	2.13	0.082	0.092	0.098	0.106	0.116	0.873	0.113
Methoxyfenozid	161050-58-4	3.7	0.056	0.063	0.057	0.069	0.070	0.749	0.068
Metolachlor	51218-45-2	3.12	0.076	0.080	0.086	0.096	0.102	0.815	0.099
Metribuzin	21087-64-9	1.7	0.083	0.100	0.096	0.112	0.119	0.934	0.117
Napropamid	15299-99-7	3.36	0.041	0.045	0.055	0.060	0.057	2.793	0.070
Nicosulfuron	111991-09-4	0.6 (−2.6)	0.019	0.021	0.022	0.022	0.022	2.304	0.023
Pirimicarb	23103-98-2	1.7	0.077	0.086	0.089	0.102	0.107	0.988	0.106
Propamocarb	24579-73-5	0.8 (−0.7)	0.017	0.019	0.022	0.021	0.020	5.044	0.024
Propyzamid	23950-58-5	3.43	0.044	0.051	0.058	0.068	0.063	2.891	0.079
Pyrimethanil	53112-28-0	2.8	0.024	0.025	0.028	0.038	0.031	6.475	0.043
Spiroxamin	118134-30-8	2.9	0.034	0.041	0.035	0.037	0.040	0.553	0.038
Sulfamethoxazole	723-46-6	0.89	0.040	0.046	0.042	0.048	0.048	1.008	0.048
Tebuconazol	107534-96-3	3.7	0.045	0.052	0.060	0.072	0.067	2.820	0.086
Terbuthylazine	5915-41-3	3.21	0.063	0.072	0.079	0.089	0.089	1.612	0.098
Terbutryn	886-50-0	3.74	0.050	0.057	0.063	0.075	0.071	2.321	0.084
Thiacloprid	111988-49-9	1.3	0.058	0.072	0.073	0.086	0.084	1.898	0.095
Thiamethoxam	153719-23-4	−0.1	0.075	0.089	0.086	0.099	0.104	0.967	0.104

[a] Partition coefficients in brackets are normalized to the fraction of the neutral species at pH 8 using $D_{OW}(pH\ 8) = 1 / (1 + 10^{(8-pKa)})K_{OW}$.

day^{-1}) to bring the water concentration to the desired level (1 μg L^{-1}). The nominal concentration of 1 μg L^{-1} was chosen in order to have enough analyte on the samplers even after a single day of deployment. As freshwater was continuously added to the system, a peristaltic pump was installed to spike the water with the target compounds (dissolved in methanol) and to maintain the desired concentration. To monitor the water concentration during calibration, 100 mL of water were sampled every hour from the system using an automated refrigerated sampler (ISCO 6712FR). Samples were then combined to obtain one composite sample per 24 h. These composite water samples were prepared for direct injection by adding 100 μL of internal standards solution (in acetonitrile) and 100 μL of acetonitrile to 800 μL of the composite water sample (for a total volume of 1000 μL).

Water flow velocities were set constant in the 4 channels at approximatively 5, 12, 20 and 40 cm s^{-1}. Alabaster-based k_w were measured to characterize hydrodynamics at the surface of the samplers (4 measures per channel) (Glanzmann et al., 2022). Briefly, the mass loss of alabaster (Δm in g) was determined by weighing alabaster plates before and after exposure in the channels for 1 to 5 h, depending on the flow velocity. The mass transfer coefficient of the WBL for $CaSO_4$ ($k_{w,CaSO4}$ in dm day^{-1}) was then determined using the method proposed by Booij et al. (2017):

$$k_{w,CaSO4} = \frac{\Delta m}{AtC_w^*} \quad (1)$$

where A (dm^2) is the surface area of the plate, t (days) is time and C_w (g L^{-1}) is the alabaster solubility in water calculated from background concentrations of calcium and sulfate (O'Brien et al., 2011b). The k_w for organic compounds ($k_{w,org}$) were then calculated using the following equation:

$$k_{w,org} = k_{w,CaSO4}\left(\frac{D_{w,org}}{D_{w,CaSO4}}\right)^{2/3} \quad (2)$$

where $D_{w,org}$ is the diffusion coefficient in water at experimental temperature for the organic compound (m^2 s^{-1}) estimated from McGowan molar volumes as suggested by Schwarzenbach et al. (2016), and using the temperature effect as predicted by Hayduk and Laudie (1974). $D_{w,CaSO4}$ is the diffusion coefficient in water at experimental temperature for $CaSO_4$ (m^2 s^{-1}) obtained from Li and Gregory (1974).

2.4. Passive sampler calibration experiment

SDB-RPS disks and PES membranes were preconditioned by immersion in methanol for 30 min and then in Milli-Q water for at least 30 min (Vermeirssen et al., 2009; Estoppey et al., 2019). They were mounted in duplicates between stainless steel plates with a one-sided exposed area of 12.6 cm^2 as presented on SI, Fig. S1.3. A total of 56 passive samplers (extraction disks and PES membranes) were prepared and kept in milli-Q water (4 °C) until deployment. They were then mounted on the stainless-steel holders and were deployed in duplicate in the 4 channels for 7 different exposure durations (1, 2, 4, 8, 12, 15 and 21 days). They were suspended in the channels at mid-height and parallel to the flow (SI, Fig. S1.4), exactly at the same positions as during k_w measurements. After exposure, SDB-RPS disks and PES membranes were removed from the holder, dried with aluminum sheets, and put into individual 10 mL amber glass vials. Seven milliliters of acetone were added and the vials were kept in the freezer (−24 °C). Six additional control samplers were prepared following the same protocol, but instead of being immersed in water they were stored in the fridge (4 °C) as field controls.

2.5. Extraction

The vials were allowed to reach room temperature (30 min) before starting the extraction. Then they were placed on a rotatory shaker for 30 min at 30 rpm. The acetone was transferred to clean 20 mL vials and, membranes and disks were extracted a second time (30 min, 30 rpm) with 7 mL of methanol. Acetone and methanol from both extractions were combined in the 20 mL vials. The 14 mL extracts were kept in the freezer (−24 °C) until analysis. Passive sampler extracts were prepared with 800 μL of Milli-Q water, 100 μL of extract and 100 μL of internal standards solution (in acetonitrile).

2.6. Chemical analysis

Analytes were quantified by high-performance liquid chromatography coupled to tandem mass spectrometry using electrospray as an ionization source (HPLC-ESI-MS/MS, QTRAP 6500+, AB Sciex). Separation was carried out on a Phenomenex Luna Omega column (2.1 × 150 mm, 1.6 μm). Milli-Q water and acetonitrile, both acidified with 0.1 % formic acid, were used as mobile phases for chromatographic separation. The analytical method parameters are detailed in SI, Table S2.1. Limits of detection and quantification have been determined empirically by analyzing samples prepared with decreasing concentrations of analytes (Armbruster and Pry, 2008) (SI, Table S2.3).

2.7. Data analysis

The R_S (in L day^{-1}) were determined using the equivalent sampled volume (V_e, in L), which is the mass of analytes extracted from SDB disks (N_s in ng) divided by the average water concentration of the analyte (C_w in ng L^{-1}) during the sampling period of each sampler ($V_e = N_s / C_w$). The uptake data were fitted with the *sampling rate model* (Huckins et al., 2006) using the unweighted non-linear least-squares (NLS) method. NLS fitting was done with spreadsheet operations using the solver function in Microsoft Excel (Billo, 2001; Booij and Smedes, 2010). This widely used first-order uptake model describes the contaminant uptake rate as linearly proportional to the concentration difference between the water and the sorbent:

$$V_e = m\,K_{SW}\left(1 - \exp\left(-\frac{R_S\,t}{m\,K_{SW}}\right)\right) \quad (3)$$

where m is the mass of the receiving phase of the passive sampler (kg), K_{SW} is the sampler-water partition coefficient (L kg^{-1}), and t is the time (days). For small t, Eq. (3) approaches:

$$V_e = R_S\,t \quad (4)$$

Then, for each compound, the R_S obtained in the four channels have been plotted against the previously measured k_w. The following MRC model was fitted to these data by minimizing relative errors on R_S, with $R_{S,max}$ as the only adjustable parameter:

$$\frac{1}{R_S} = \frac{1}{A k_w} + \frac{1}{R_{S,max}} \quad (5)$$

with A being the area of the sampler ($A = 0.126$ dm^2). Finally, this model has been adapted to better describe the obtained calibration data by introducing a fitting parameter.

3. Results and discussion

3.1. Analyte concentrations in water

Aqueous concentrations of compounds spiked into the recirculated water were measured between 0.25 and 1.2 μg L^{-1} during the calibration experiment (SI, Table S3.1). Most of those concentrations were much lower than the target concentration (1 μg L^{-1}) and they tended to decrease with time. This could be due to adsorption or degradation of the compounds in the system. However, aqueous concentrations remained stable enough during the experiment (RSD < 15 %).

3.2. Accumulation in PES membrane and SDB-RPS sorbent

All the 44 compounds spiked in the water were detected in the exposed PSDs ranging in accumulated mass from 34 to 1660 ng $sampler^{-1}$ after 15 days exposure (extracted from SDB-RPS disks). These results confirm the potential of passive sampling for the qualitative assessment of hydrophilic micropollutants in surface water (Harman et al., 2012; Mills et al., 2014; Moschet et al., 2015).

Analyze of PES membranes showed that accumulation in PES is dependent on the compounds. After 21 days, 17 analytes had an $N_{s,PES}/N_{s,SDB}$ ratio higher than 1 meaning that these analytes were more significantly retained by the membrane in comparison to the retention in the SDB-RPS disk. As observed in several studies (Vermeirssen et al., 2012; Morin et al., 2018; Estoppey et al., 2019; MacKeown et al., 2022), PES sorption

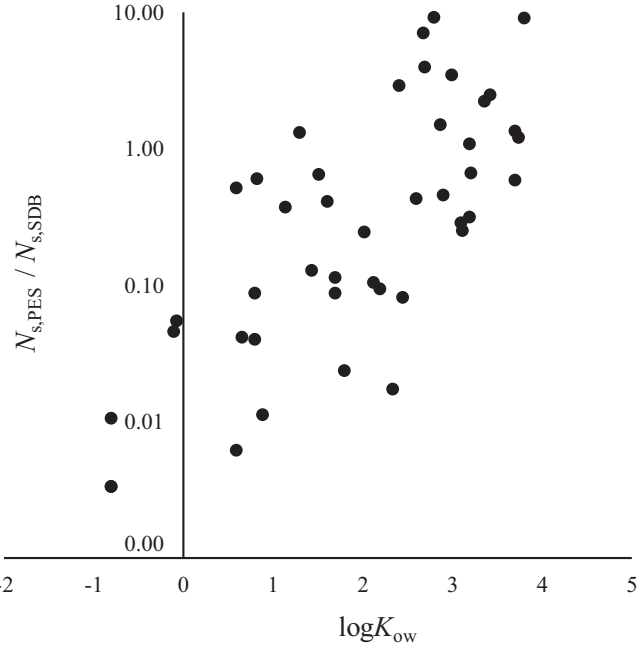

Fig. 1. Sorption in PES membrane (logarithmic scale) after 21 days as a function of the compounds $logK_{OW}$.

tended to increase with hydrophobicity (Fig. 1). However, hydrophobic interactions are not the only explanation for PES adsorption (MacKeown et al., 2022). It is likely that physicochemical characteristics also influence the accumulation on PES membrane, such as π-π interactions or hydrogen bonding through the polar sulfonyl groups (Chepchirchir et al., 2020). Estoppey et al. (2019) and Morin et al. (2018) also mentioned chlorine atoms substituted on the same phenyl group for diuron, which accumulated strongly in the membrane.

Four different uptake profiles are shown as examples in Fig. 2. Hydrophilic compounds like caffeine in Fig. 2 ($\log K_{OW} = -0.1$) only slightly accumulated in the membrane (at 21 days, $N_{s,PES} / N_{s,SDB} < 0.1$) and were quickly transferred to the SDB-RPS disk. Compounds of medium hydrophobicity like 5-methylbenzotriazole in Fig. 2 ($\log K_{OW} = 1.6$) accumulated in the PES membrane at intermediate levels (at 21 days, $N_{s,PES} / N_{s,SDB} = 0.3$) but there was no lag in the transfer from water to SDB-RPS disk. For less hydrophilic compounds ($\log K_{OW} > 2.6$) such as Diuron or Terbutryn (Fig. 2), which accumulated strongly in PES (at 21 days, $N_{s,PES} / N_{s,SDB} = 5.4$ and 0.9, respectively), a lag time was visible but it did not appear to be longer than 2 days. In previous studies, significant accumulation in the PES membrane was also reported as a source of delay in the diffusion of compounds from the water to the sorbent material. This lag phase occurs if steady state conditions across the WBL and the membrane are not rapidly established (Huckins et al., 1993; Booij et al., 2007). Vermeirssen et al. (2012) and Estoppey et al. (2019) observed that the lag phase may approach one week for the less hydrophilic compounds. However, in the present study, even if there was appreciable sorption by PES for most compounds, no significant lag phases were observed in comparison to the literature. This could be explained by the changes in water concentration during calibration (Shaw and Mueller, 2009) − especially at the beginning of the exposure − and would need further investigation.

3.3. Sampling rates (R_S)

For each compound, four different R_S – at four k_w conditions – were determined using the sampling rate model (Eq. (3)) (see Fig. 3 and SI, Section S4). The lines in Fig. 3 (and in SI, Section S4 for the other compounds) represent the uptake curves into SDB disks and demonstrate that the model fit the data well.

The R_S at day 14 were determined using the sampling rate model (Huckins et al., 2006). The adjustable parameters (R_s and K_{sw}) were firstly obtained by fitting the model (Eq. (3)) to the calibration data using NLS method to minimize residual errors. The R_S of a given compound was calculated by dividing its modelized V_e at day 14 by the time (14 days). The obtained R_S are compiled in Table 1.

The determined R_S ranged from 0.015 L day^{-1} (diazinon in channel 1) to 0.112 L day^{-1} (chloridazon in channel 4) with a median value of

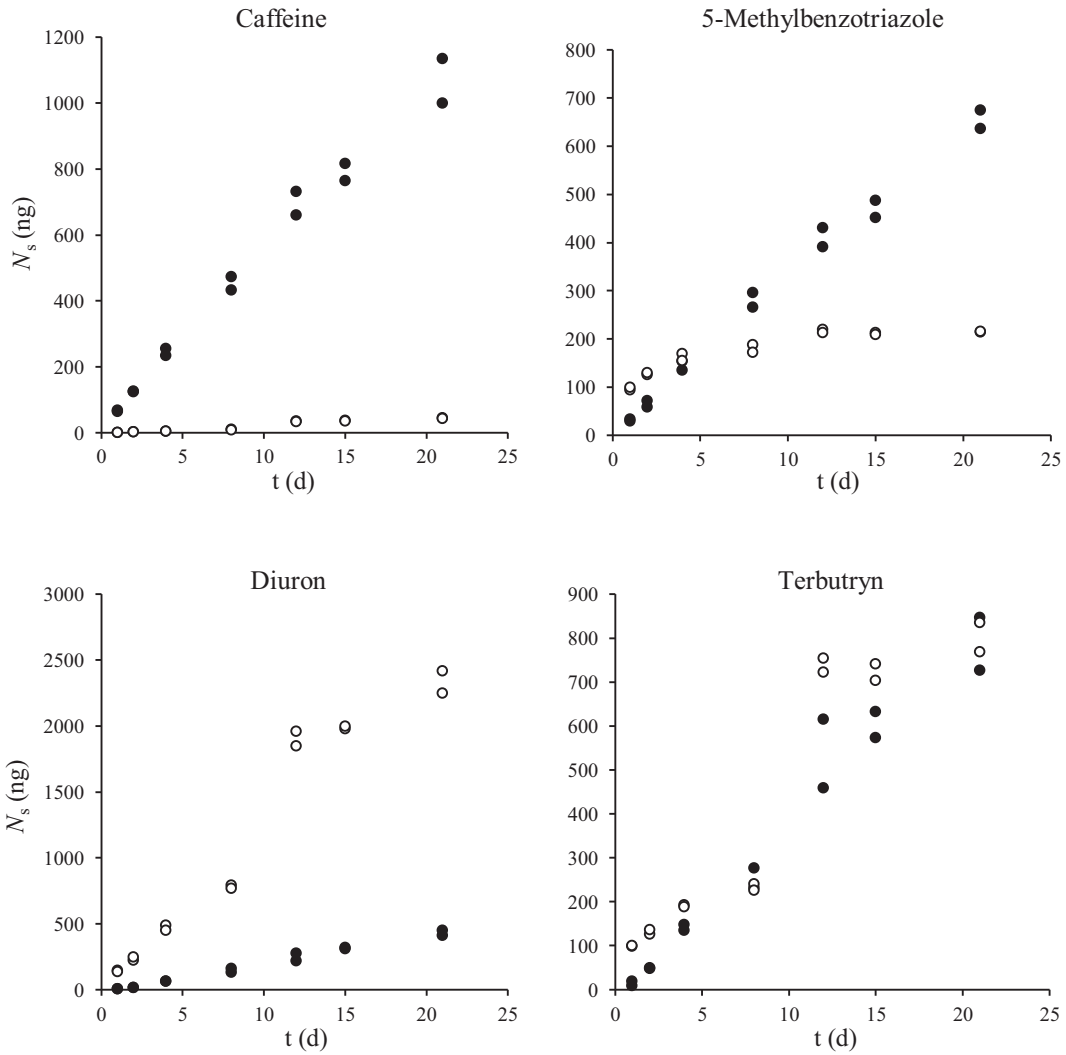

Fig. 2. Extracted amount (ng) of caffeine, 5-methylbenzotriazole, diuron and, terbutryn (channel 2, velocity of approx. 12 cm s^{-1}) from SDB disks (black circles) and PES membranes (white circles) versus time (days).

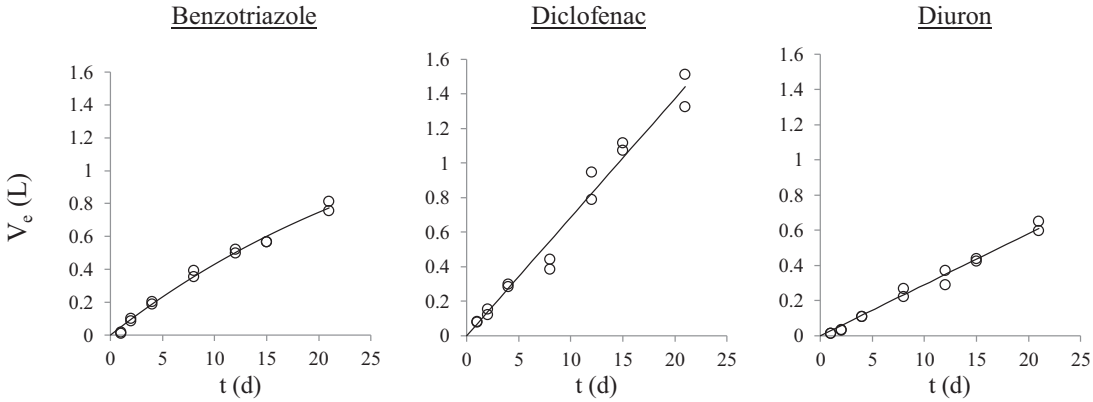

Fig. 3. Equivalent sampled volume (V_e) of benzotriazole, diclofenac, and diuron in channel 2. Solid lines are fittings using the sampling rate model (Eq. (3)). On the second row, circles are residual errors of the fitting using the sampling rate model.

0.062 L day^{-1}. These values have been compared with R_S from six previous studies using the same sampler configuration (SDB-RPS disk and PES membrane) (Shaw et al., 2009; Shaw and Mueller, 2009; Vermeirssen et al., 2009; O'Brien et al., 2011a; Vermeirssen et al., 2012; Moschet et al., 2015). Overall, the R_S shared good agreement with less than a 2-fold factor for 23 out of the 28 compared compound (SI, Fig. S5.1). For 2,4-D, diazinon, diuron, metolachlor, and sulfamethoxazole, larger differences have been observed. This could be explained by the different experimental setups, e.g. larger membrane pore size or exposure duration (Moschet et al., 2015). Indeed, a larger pore size leads to a decrease in membrane resistance which may results in higher R_S whereas differences in calibration duration is a source of variability in R_S for compounds with nonlinear uptakes.

3.4. Relationships between k_w and R_S

For most of the studied compounds, the MRC model (Eq. (5)) gives a good prediction of the observed R_S from k_w. However, as also observed by Booij and Chen (2018), the R_S obtained at the highest velocities (and thus k_w) were above the $R_{S,max}$ for several compounds (e.g., diuron and diazinon in Fig. 4) indicating that this model is not always adequate. Thus, an adapted model was tested by adding a second adjustable parameter "a" in the following semi-empirical model (adapted MRC model):

$$\frac{1}{R_S} = \frac{a}{Ak_w} + \frac{1}{R_{S,\,max}} \tag{6}$$

This model allowed for better fitting of the data (Fig. 4 and SI, Table S6.1), especially because $R_{S,max}$ is not exceeded at high k_w. The adjustable parameters estimated with the MRC model (i.e., $R_{S,max}$) and the adapted MRC model (i.e., a and $R_{S,max}$) are given in Table 1.

The compounds having more accumulation in the PES membrane than in the sorbent (e.g., diuron in Fig. 2) are less in agreement with the MRC model (Fig. 4). Indeed, the residual standard errors (RSE) in R_S tend to increase when the ratio of $N_{s,PES}$ / $N_{s,SDB}$ increases (Fig. 5). For those compounds, apparently more influenced by hydrodynamics, data were better described by the adapted model. When using this second model to fit the data, the RSE were smaller (median RSE = 0.005 L day^{-1} for MRC model and 0.003 L day^{-1} for adapted MRC model) and more randomly distributed (Fig. 5), indicating that the adapted model performed better at describing the data.

The estimated value for the parameter "a" is above 1 for 26 compounds and below 1 for the remaining 18, with an average value of 2.03 and a median value at 1.15, suggesting that the WBL resistance ($1/Ak_w$) is slightly higher than expected (see Table 1). Whereas a value smaller than 1 could be explained by a smaller WBL resistance due to the flow penetration into the PES membrane, no clear explanation has been found for an increase in WBL resistance. Further experiments, for example by testing different models at low k_w (e.g., 1 to 2 dm day^{-1}) are needed to better understand the influence of flow on WBL resistance and could explain the obtained results. The resistance of the biofilm layer to the overall mass transfer should also be further evaluated. No biofilm layer was visible in this study, but when the resistance of that layer is not negligible an additional term accounting for this resistance should be added in Eqs. (5) and (6).

The R_S obtained in the four channels almost reached a plateau and did not increase much with k_w in the studied range (k_w approx. 3–9 dm day^{-1}) for 31 compounds (e.g. 5-methylbenzotriazole and caffeine in Fig. 4). This is likely because the uptake is mostly controlled by the membrane at these hydrodynamic conditions. As suggested by the fits (Fig. 4) and previous studies, water flow velocity should have more impact on R_S at smaller k_w (Vermeirssen et al., 2009; O'Brien et al., 2011a). This could be confirmed by calibrating PSDs at smaller k_w. For 13 compounds (boscalid, chlorotoluron, diazinon, diuron, ethofumesate, metalaxyl-M, napropamid, nicosulfuron, propamocarb, propyzamid, pyrimethanil, tebuconazol, terbutryn), R_S was more impacted by hydrodynamics (R_S increased with k_w). All these compounds have a value higher than 2 for the adjustable parameter a with the adapted MRC model.

3.5. Implications and field application

The established relationships between k_w and R_S allow determining site-specific sampling rates based on in-situ measurements of k_w. As long as there is no better understanding of the uptake mechanisms, the authors suggest to use the proposed semi-empirical model (adapted MRC model) with the reported parameters for the determination of in-situ R_S. Those parameters (a and $R_{S,max}$) can be used for similar PSD and similar field conditions (e.g., temperature and pH). Choosing the most accurate R_S regarding the hydrodynamic conditions will therefore help provide better TWA concentrations from amounts extracted from the samplers using $C_w = \frac{N_S}{R_S\, t}$. In rivers, this can be done by the co-deployment of PRC-spiked silicone disks in parallel to the hydrophilic passive samplers. The suggested method was tested in a Swiss river, and part B of this study presents the results and evaluates its field application.

As the R_S provided in this study – as well as the proposed models' parameters – have been determined for a sampling period of 14 days, and because uptake is not fully linear, it is better to stick to this duration when applying the proposed methodology. However, for most compounds, the linearity of uptake is good and thus a variation of a few days will not make a big difference in the R_S and thus in the calculated TWA concentrations.

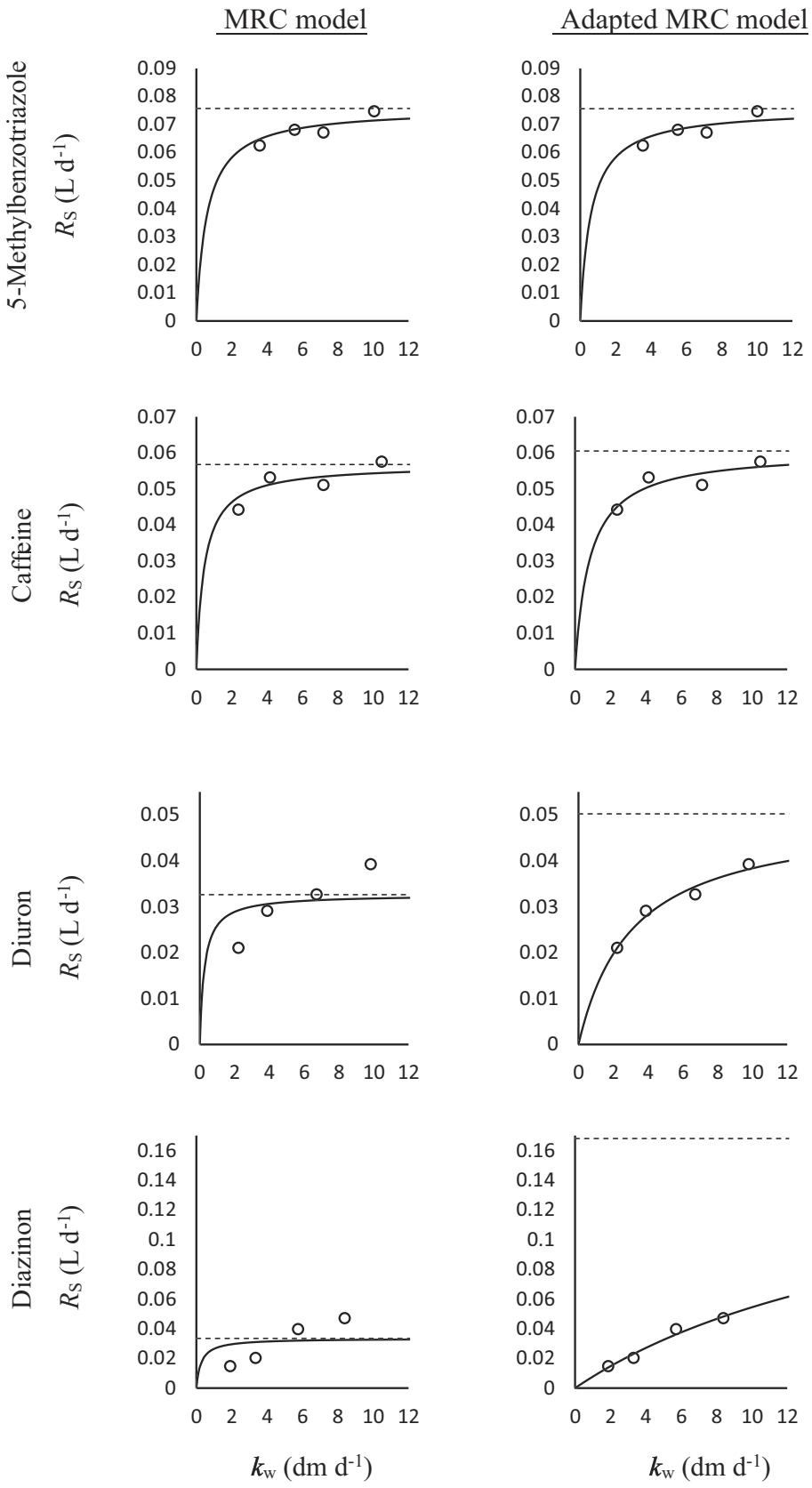

Fig. 4. Sampling rates (R_S) of 5-methylbenzotriazole, caffeine, diuron, and diazinon as a function of mass transfer coefficient of the water boundary layer (k_w). The solid lines represent the fitting to the data using the MRC model and the adapted MRC model. Dashed lines are the estimated maximum sampling rates ($R_{S,max}$).

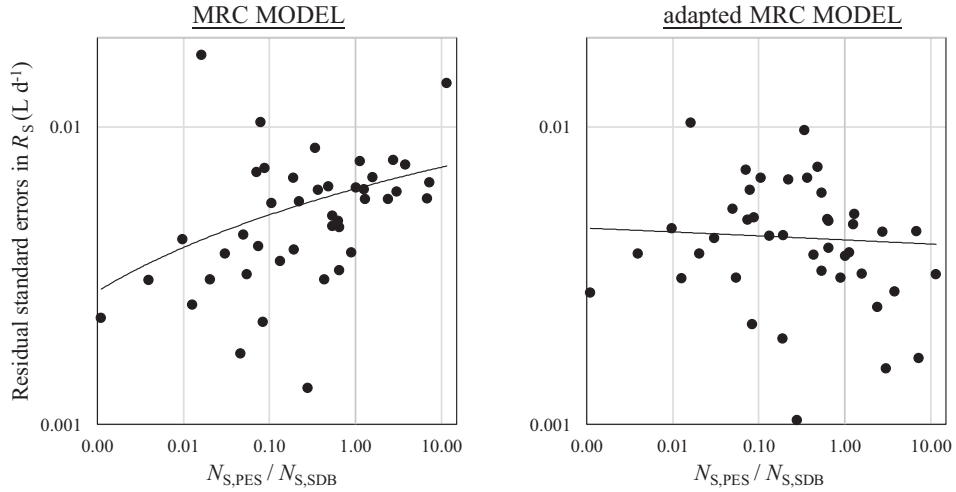

Fig. 5. Residual standard errors in R_S (L day^{-1}) for the studied compounds (n = 44) using fittings with the MRC model and the adapted MRC model. Black lines are the logarithmic regressions (y = a ln(x) + b).

CRediT authorship contribution statement

Vick Glanzmann: Conceptualization, Methodology, Investigation, Formal analysis, Data curation, Visualization, Writing – original draft, Writing – review & editing. **Naomi Reymond:** Investigation, Formal analysis. **Céline Weyermann:** Supervision, Conceptualization, Writing – review & editing. **Nicolas Estoppey:** Supervision, Conceptualization, Methodology, Writing – review & editing.

Data availability

Data will be made available on request.

Declaration of competing interest

The authors declare that they have no known competing financial interests or personal relationships that could have appeared to influence the work reported in this paper.

Acknowledgements

The authors wish to thank Dr. Kees Booij (PaSOC, The Netherlands) for his precious support during data treatment. They also wish to thank Dr. Etiënne L.M. Vermeirssen (Oekotoxzentrum Eawag-EPFL, Switzerland) for his advice in designing the stainless steel housing.

Appendix A. Supplementary data

Supplementary data to this article can be found online at https://doi.org/10.1016/j.scitotenv.2023.162037.

References

Alvarez, D.A., Stackelberg, P.E., Petty, J.D., Huckins, J.N., Furlong, E.T., Zaugg, S.D., Meyer, M.T., 2005. Comparison of a novel passive sampler to standard water-column sampling for organic contaminants associated with wastewater effluents entering a New Jersey stream. Chemosphere 61, 610–622.

Armbruster, D.A., Pry, T., 2008. Limit of blank, limit of detection and limit of quantitation. Clin.Biochem.Rev. 29, S49.

Behmel, S., Damour, M., Ludwig, R., Rodriguez, M.J., 2016. Water quality monitoring strategies — a review and future perspectives. Sci. Total Environ. 571, 1312–1329.

Billo, E.J., 2001. Non-linear regression using the solver. Excel for Chemists: A Comprehensive Guide. John Wiley & Sons, Inc, New York, pp. 223–238.

Booij, K., Chen, S., 2018. Review of atrazine sampling by polar organic chemical integrative samplers and Chemcatcher. Environ. Toxicol. Chem. 37, 1786–1798.

Booij, K., Maarsen, N.L., Theeuwen, M., van Bommel, R., 2017. A method to account for the effect of hydrodynamics on polar organic compound uptake by passive samplers. Environ. Toxicol. Chem. 36, 1517–1524.

Booij, K., Smedes, F., 2010. An improved method for estimating in situ sampling rates of nonpolar passive samplers. Environ. Sci. Technol. 44, 6789–6794.

Booij, K., Vrana, B., Huckins, J.N., 2007. Theory, modelling and calibration of passive samplers used in water monitoring. In: Greenwood, R., Mills, G.A., Vrana, B. (Eds.), Passive Sampling Techniques in Environmental Monitoring. Elsevier, Amsterdam, pp. 141–169.

Chepchirchir, B.S., Zhou, X., Paschke, A., Schüürmann, G., 2020. Polyethersulfone as suitable passive sampler for waterborne hydrophobic organic compounds – laboratory calibration and field test in the Sosiani river, Kenya. Sci. Total Environ. 699, 134056.

Doppler, T., Mangold, S., Wittmer, I., Spycher, S., Stamm, C., Singer, H., Junghans, M., Kunz, M., 2017. Hohe Pflanzenschutzmittelbelastung in Schweizer Bächen. Aqua & Gas 4/2017, 46 56.

Estoppey, N., Mathieu, J., Gascon Diez, E., Sapin, E., Delémont, O., Esseiva, P., de Alencastro, L.F., Coudret, S., Folly, P., 2019. Monitoring of explosive residues in lake-bottom water using Polar Organic Chemical Integrative Sampler (POCIS) and Chemcatcher: determination of transfer kinetics through polyethersulfone (PES) membrane is crucial. Environ. Pollut. 252, 767–776.

Fang, W., Peng, Y., Muir, D., Lin, J., Zhang, X., 2019. A critical review of synthetic chemicals in surface waters of the US, the EU and China. Environ. Int. 131, 104994.

Fauvelle, V., Kaserzon, S.L., Montero, N., Lissalde, S., Allan, I.J., Mills, G., Mazzella, N., Mueller, J.F., Booij, K., 2017. Dealing with flow effects on the uptake of polar compounds by passive samplers. Environ. Sci. Technol. 51, 2536–2537.

Glanzmann, V., Booij, K., Reymond, N., Weyermann, C., Estoppey, N., 2022. Determining the mass transfer coefficient of the water boundary layer at the surface of aquatic integrative passive samplers. Environ. Sci. Technol. 56, 6391–6398.

Harman, C., Allan, I.J., Bäuerlein, P.S., 2011. The challenge of exposure correction for polar passive samplers—the PRC and the POCIS. Environ. Sci. Technol. 45, 9120–9121.

Harman, C., Allan, I.J., Vermeirssen, E.L.M., 2012. Calibration and use of the polar organic chemical integrative sampler—a critical review. Environ. Toxicol. Chem. 31, 2724–2738.

Hayduk, W., Laudie, H., 1974. Prediction of diffusion coefficients for nonelectrolytes in dilute aqueous solutions. AIChE J. 20, 611–615.

Hirsch, R.M., Hamilton, P.A., T.L., M., 2006. U.S. Geological Survey perspective on water-quality monitoring and assessment. J. Environ. Monit. 8, 512–518.

Huckins, J.N., Manuweera, G.K., Petty, J.D., Mackay, D., Lebo, J.A., 1993. Lipid-containing semipermeable membrane devices for monitoring organic contaminants in water. Environ. Sci. Technol. 27, 2489–2496.

Huckins, J.N., Petty, J.D., Booij, K. (Eds.), 2006. Monitors of Organic Chemicals in the Environment: Semipermeable Membrane Devices New York.

Langer, M., Junghans, M., Spycher, S., Koster, M., Baumgartner, C., Vermeissen, E., Werner, I., 2017. Hohe ökotoxikologische Risiken in Bächen. Aqua Gas 97, 58–68.

Li, H., Vermeirssen, E.L.M., Helm, P.A., Metcalfe, C.D., 2010. Controlled field evaluation of water flow rate effects on sampling polar organic compounds using polar organic chemical integrative samplers. Environ. Toxicol. Chem. 29, 2461–2469.

Li, Y.-H., Gregory, S., 1974. Diffusion of ions in sea water and in deep-sea sediments. Geochim. Cosmochim. Acta 38, 703–714.

Lissalde, S., Charriau, A., Poulier, G., Mazzella, N., Buzier, R., Guibaud, G., 2016. Overview of the Chemcatcher® for the passive sampling of various pollutants in aquatic environments part B: field handling and environmental applications for the monitoring of pollutants and their biological effects. Talanta 148, 572–582.

Lissalde, S., Mazzella, N., Fauvelle, V., Delmas, F., Mazellier, P., Legube, B., 2011. Liquid chromatography coupled with tandem mass spectrometry method for thirty-three pesticides in natural water and comparison of performance between classical solid phase extraction and passive sampling approaches. J. Chromatogr. A 1218, 1492–1502.

MacKeown, H., Benedetti, B., Scapuzzi, C., Di Carro, M., Magi, E., 2022. A review on polyethersulfone membranes in polar organic chemical integrative samplers: preparation, characterization and innovation. Crit. Rev. Anal. Chem. 1–17.

Mills, G.A., Gravell, A., Vrana, B., Harman, C., Budzinski, H., Mazzella, N., Ocelka, T., 2014. Measurement of environmental pollutants using passive sampling devices - an updated commentary on the current state of the art. Environ. Sci. Process. Impacts 16, 369–373.

Morin, N.A.O., Mazzella, N., Arp, H.P.H., Randon, J., Camilleri, J., Wiest, L., Coquery, M., Miège, C., 2018. Kinetic accumulation processes and models for 43 micropollutants in "pharmaceutical" POCIS. Sci. Total Environ. 615, 197–207.

Moschet, C., Vermeirssen, E.L.M., Singer, H., Stamm, C., Hollender, J., 2015. Evaluation of in-situ calibration of Chemcatcher passive samplers for 322 micropollutants in agricultural and urban affected rivers. Water Res. 71, 306–317.

Mutzner, L., Bohren, C., Mangold, S., Bloem, S., Ort, C., 2020. Spatial differences among micropollutants in sewer overflows: a multisite analysis using passive samplers. Environ. Sci. Technol. 54, 6584–6593.

Mutzner, L., Vermeirssen, E.L.M., Mangold, S., Maurer, M., Scheidegger, A., Singer, H., Booij, K., Ort, C., 2019. Passive samplers to quantify micropollutants in sewer overflows: accumulation behaviour and field validation for short pollution events. Water Res. 160, 350–360.

O'Brien, D., Bartkow, M., Mueller, J.F., 2011a. Determination of deployment specific chemical uptake rates for SDB-RPD Empore disk using a passive flow monitor (PFM). Chemosphere 83, 1290–1295.

O'Brien, D.S., Booij, K., Hawker, D.W., Mueller, J.F., 2011b. Method for the in situ calibration of a passive phosphate sampler in estuarine and marine waters. Environ. Sci. Technol. 45, 2871–2877.

Salim, F., Górecki, T., 2019. Theory and modelling approaches to passive sampling. Environ. Sci. Process. Impacts 21, 1618–1641.

Schwarzenbach, R., Egli, T., T.B., H., von Gunten, U., Wehrli, B., 2010. Global water pollution and human health. Annu. Rev. Environ. Resour. 35, 109–136.

Schwarzenbach, R.P., Gschwend, P.M., Imboden, D.M., 2016. Environmental Organic Chemistry. 3rd ed. John Wiley & Sons, Hoboken, NJ, USA.

Schymanski, E.L., Singer, H.P., Longrée, P., Loos, M., Ruff, M., Stravs, M.A., Ripollés Vidal, C., Hollender, J., 2014. Strategies to characterize polar organic contamination in wastewater: exploring the capability of high resolution mass spectrometry. Environ. Sci. Technol. 48, 1811–1818.

Shaw, M., Eaglesham, G., Mueller, J.F., 2009. Uptake and release of polar compounds in SDB-RPS Empore™ disks; implications for their use as passive samplers. Chemosphere 75, 1–7.

Shaw, M., Mueller, J.F., 2009. Time integrative passive sampling: how well do chemcatchers integrate fluctuating pollutant concentrations? Environ. Sci. Technol. 43, 1443–1448.

Spycher, S., Mangold, S., Doppler, T., Junghans, M., Wittmer, I., Stamm, C., Singer, H., 2018. Pesticide risks in small streams—how to get as close as possible to the stress imposed on aquatic organisms. Environ. Sci. Technol. 52, 4526–4535.

Vermeirssen, E.L.M., Asmin, J., Escher, B.I., Kwon, J.-H., Steimen, I., Hollender, J., 2008. The role of hydrodynamics, matrix and sampling duration in passive sampling of polar compounds with EmporeTM SDB-RPS disks. J. Environ. Monit. 10, 119–128.

Vermeirssen, E.L.M., Bramaz, N., Hollender, J., Singer, H., Escher, B.I., 2009. Passive sampling combined with ecotoxicological and chemical analysis of pharmaceuticals and biocides – evaluation of three Chemcatcher™ configurations. Water Res. 43, 903–914.

Vermeirssen, E.L.M., Dietschweiler, C., Escher, B.I., van der Voet, J., Hollender, J., 2012. Transfer kinetics of polar organic compounds over polyethersulfone membranes in the passive samplers POCIS and Chemcatcher. Environ. Sci. Technol. 46, 6759–6766.

Vrana, B., Allan, I.J., Greenwood, R., Mills, G.A., Dominiak, E., Svensson, K., Knutsson, J., Morrison, G., 2005. Passive sampling techniques for monitoring pollutants in water. TrAC Trends Anal. Chem. 24, 845–868.